Inkjetprinting of Vertically Integrated RC-Circuits

Dietrich Jeschke and Klaus Krüger, University of the Federal Armed Forces (Germany)

Abstract

Both capacitors and resistors are widely used passive components. Considering micro hybrid circuits printing of both devices is required. Striving for space-saving layouts, multi-layer capacitors are requested. Additionally, vertical integration of devices is desirable. However, today's screen printing technology cannot be applied to uneven surfaces, limiting the aspect ratio and the ability of vertical integration. Thus, usually SMD capacitors are preferred. In order to increase the degree of vertical integration, resistors are printed on top of printed capacitors, creating RC-circuits. The mask-less inkjet printing allows for realization of such structures. To keep the process simple, no in-between-sintering is applied; the entire component is co-fired in one final step.

To model the electric behavior of the RC-circuits, both the capacitors' and resistors' behavior is compared to non-integrated devices of the same size and shape. Based on these results, it is shown how existing single-device models can be applied to integrated devices.

To improve the sintering process, furthermore the impact of heat on the behavior of the used organic additives is examined. The solid additives have to burn thoroughly. It is analyzed whether there is a liquid phase during sintering and how this may affect the resulting structure.

State of Research

The printing of thickfilm capacitors using inkjet has come a long way from first feasibility studies [1] to in-depth analysis of their production and electrical behavior [2]. The latest research concerns in-situ blending of inks to adjust resistivity [3, 4]. In parallel, other passive components as capacitors and inductors have been implemented [5], with the latest research concerning capacitors due to their higher importance. It has been shown, that vertical integration of capacitors is possible and that they can be sintered in a single step [6]. However, up to now inkjet print the different types of passive devices has been examined separately. A combination of different devices has not been considered yet.

Motivation

In electronics, the big trend of the last decades is the ever decreasing size of components. But while the shrinkage of information carrying structures is only limited by manufacturing technology, devices for power applications cannot shrink below their physical limits that are determined by conductor resistivity and heat dissipation. Therefore, in power applications thick film passives printed with inkjet technology can be a viable option.

Another big trend in industry is the trend of mass customization. Currently power components are mass produced using standardized modules. Since inkjet printing is compatible with all generic levels of mass customization, it creates new possibilities of flexible mass production. To incorporate the process inherent flexibility, common architectures for potential product families have to be developed [7].

A first step into this direction is to evaluate the feasibility of printing a simple RC-circuit that can be varied in both capacity and resistivity while not changing the substrate area used or the geometry of the galvanic interfaces to possible components above and beneath the RC-circuit.

Design

For the heat dissipation needed for power applications, the structure is printed on Al_2O_3 substrates due to their high thermal conductivity. All contacts have to be on the upper respective lower face for real 3D-intergation. The horizontal dimensions have to be independent of the electric behavior.

To achieve those requirements, the capacitor design of previous research [6] is used. **Figure 1** shows how an added connective layer topped by the capacitor creates a three pole RC-circuit, that can be used either as a high or low pass, depending on the way it is incorporated into larger circuits. The number of repetitions r shows how many copies of the shown structure are stacked vertically, thus setting the resistivity of resistors and the capacity of the capacitors.

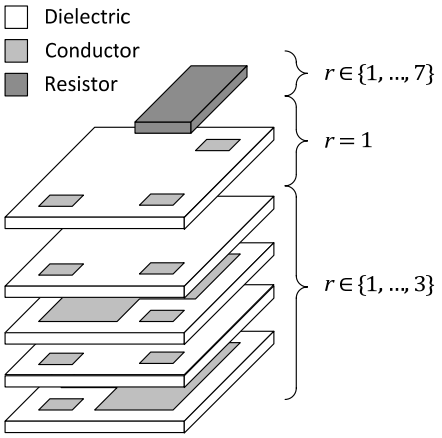

Figure 1: *Principal design of the RC-component.*

Each layer in the picture is functional layer. Each functional layer is manufactured using a number n_f of printed layers. This number is determined using the targeted amount of material per area μ_A, the drop mass m_D, the solid substance content ϕ and the printing pitch α

$$n_f = \frac{\mu_A}{m_D \cdot \phi \cdot \alpha^2}. \qquad (1)$$

Thus the software that creates the printing patterns calculates the number of printed layers according to the targeted amount of

material that is needed for a conductive electrode or an insulating dielectric using this process data. Each functional layer contains both, silver and $BaTiO_3$, in the ratio needed to ensure a flat surface to print on next. The number of layers for the nonfunctional material n_n is calculated using the bulk densities ρ and sinter shrinkage s of both the functional (index f) and the nonfunctional (index n) material

$$n_n = \frac{\rho_n \cdot (1 - s_n)}{\rho_f \cdot (1 - s_f)} \cdot \frac{m_{A,f}}{m_D \cdot \phi \cdot \alpha^2}. \qquad (2)$$

Two general substrate layouts were used. The first substrate layout just contains single capacitors without resistors and is used to improve the manufacturing process towards low failure rates before producing RC-circuits. The second layout contains every combination of the elements shown in Figure 1. The combinations vary in the numbers of stacked capacitors (up to three) and parallel resistors (up to seven), resulting in 21 different RC-circuits.

Printing System

To print complex structures in a reproducible way it is necessary to keep the essential process parameters stable. Since the main parameter is the size and therefore the mass of a single created drop, all factors influencing the drop size have to be managed using closed loop control systems.

Drop formation in inkjet systems is a function of a number of parameters [8] shown in **Table 1**. The parameters are classified whether they are functions of the print system or the ink.

Although every physical parameter shows some temperature dependence, only viscosity shows big changes for relatively small changes in temperature. Therefore the implementation of closed loop temperature control is a key component for ink management [4, 6].

Table 1: Parameters influencing drop formation and their dependencies.

Parameter	Function of
Compressibility	Ink
Speed of Sound	Ink
Density	Ink
Viscosity	Ink, Temperature
Surface Tension	Ink
Static Pressure	Process

Controlling the static pressure is not just a necessary addition for creating reproducible states of the process system but also a requirement by the printhead used [9]. So both inlet and outlet of the printing system are equipped with pressure sensors. Each sensor is combined with a pump and a controller, so that inlet and outlet pressure can be controlled independently, creating a stable pressure gradient inside the printhead.

Inks

Due to the high density of silver particles the stability of silver inks is difficult to achieve. Silver inks used in previous research [6] containing 300 nm silver particles proved to be not stable enough to print the complex structures needed here.

Therefore 50 nm silver is used. The smaller particles are very stable but lowering particle size by the same solid substance content decreases particle distance so that the particles start to interact. This results in a strong non-Newtonian behavior of the ink. This behavior can be made more Newtonian by decreasing solid substance content, as can be seen in **Figure 2**.

The price for increased stability of the ink is a low solid substance content and an increased content of ethyl cellulosis needed to keep the viscosity of the ink at the 11.9 mPas required by the printhead manufacturer [9].

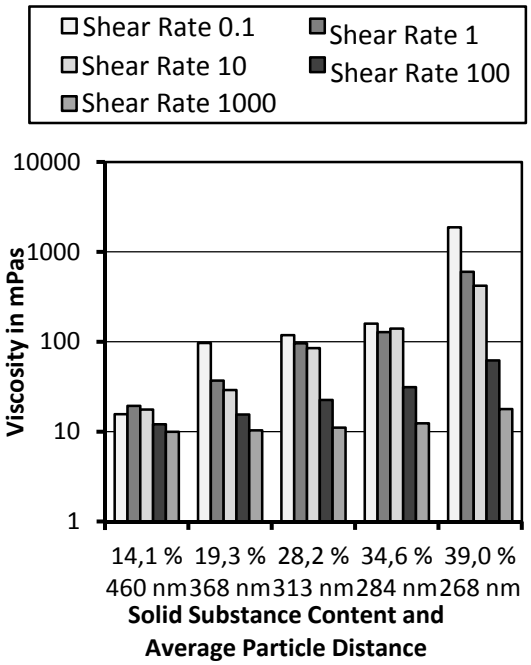

Figure 2: *Dependency of the Newtonian behavior from the solid substance content.*

For the dieletric, the $BaTiO_3$ ink of previous research was chosen [6].

Process Stability

A stable printing process is necessary to ensure that the targeted amount of material is applied by printing the calculated number of layers using eqs. (1) and (2). All the parameters of Table 1 have to be kept stable by both using closed loop controls and stable inks.

Figure 3 shows the drop weight and the solid substance amount per drop for both materials used over a period of two days. The process parameters static influx/efflux pressure and temperature were kept inside a range of ± 3 mbar respective ± 0.2 K.

As can be seen, the silver ink is extremely stable while the $BaTiO_3$ ink tends to increase in solid substance content and therefore in drop weight. This is an indication for particle sedimentation inside the printhead, since the measurements were taken after a pause in printing.

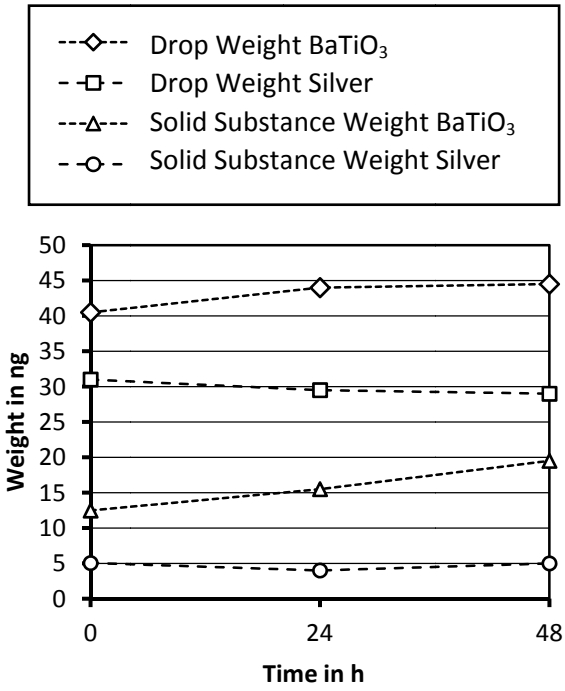

Figure 3: *Drop weight and solid substance amount for a period of 48 h.*

Using Stokes law to estimate sedimentation speed [10]

$$v_s = \frac{1}{18} \cdot (\rho_P - \rho_F) \frac{g \cdot d^2}{\eta} \qquad (3)$$

both inks should show stability in the same order of magnitude. However the $BaTiO_3$ paste used to produce the ink disperses only when stirred over very long periods of time. So the observed instability can be attributed to undissolved agglomerates of $BaTiO_3$ particles that have an increased diameter d and therefore a much higher sedimentation velocity v_s.

Drying

For drying a closed loop temperature control of the environment is used [6]. To prevent unwanted particle movement, before printing a following layer the printed structure has to by dry enough to stay in shape. This however does not mean that the organic vehicle of the ink is dried completely in each step.

The volume reduction caused by removing the vehicle too fast can result in unwanted vertical cracks of the printed structure (**Figure 4**).

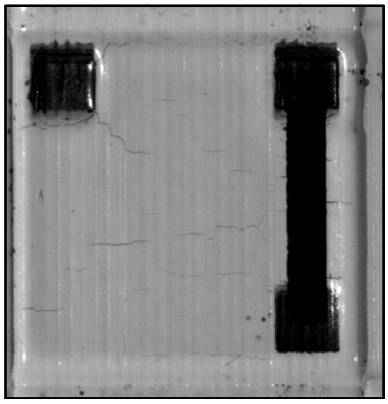

Figure 4: *Unsintered RC-circuit with drying related cracks.*

A strong hind for the influence of drying on the failure rates is the comparison of the failure rates of capacitors on single capacitor substrates with RC-circuit substrates, which also contain some single capacitors. Although both sets of structures have single capacitors with the same geometry, they differ in failure rate after similar sintering (10 % for single capacitor substrates vs. 36 % for RC-circuit substrates). The only difference is that the single capacitors on the substrates with mixed structures remained much longer in the temperature regulated environment until the stacked capacitors finished their additional printing steps.

Figure 5 shows in comparison the observed failure rates for stacked capacitors with the expected failure rates calculated on the measured failure rates for single capacitors. It also hinds at how drying influences the failure rates. The fact that the observed failure rates slightly decreases from the middle to the last column can be explained by the fact, that the RC-circuits with five capacitors are removed from the drying environment directly after finishing printing, so there is no unneeded additional drying time for them. Based on the observed failure rate of the fivefold stacked capacitor, single capacitor failure rates are 13 %, which is close to the observed 10 % for single capacitor substrates.

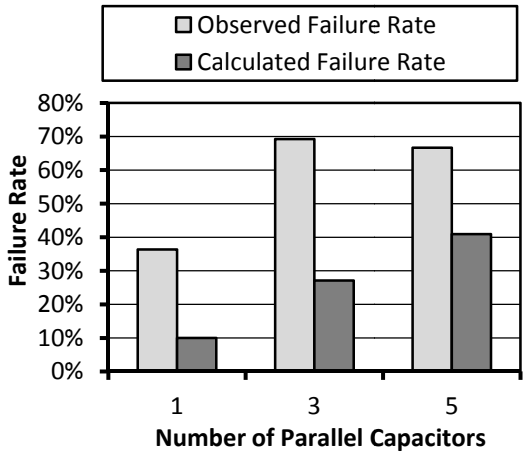

Figure 5: *Increased failure rates due to longer residence in drying environment.*

The probable mechanism behind this observation is the increased volume stream of evaporating solvent in the drying environment. If this stream exceeds the permeability of the printed structure, this results in additional crack building.

This mechanism also explains the observation of increased drying speed with increased number of layers. Parts of the vehicle do not dry on the surface but move into the already printed structure beneath. Therefore the later printed layer seems to dry quicker. This very liquid then vaporizes inside the structure forming the cracks and increasing failure rates.

The same effect applies for the printed resistors. While resistors with up to three functional layers (with each two printed layers) show the expected electrical behavior, higher resistors also show cracks that randomly increase resistivity. Therefore those resistors had to be removed from the samples.

Surface Adhesion

Another cause for cracks especially at the vertical interconnect accesses (via) is the volume reduction of the sintering silver. These cracks can be reduced by increasing the adhesive forces that tie the printed structure to the substrate.

In previous research [4, 6] the substrates were always coated with a polymer to increase the contact angle and therefore reduce the size of the spot on the substrate. The silver used sintered at temperatures high enough to adhere to the substrate after the pyrolysis of the additive.

The now used 50 nm silver starts to sinter at much lower temperatures with the polymerized surface still intact. This reduces adhesion to a large degree and causes cracks in the vias. This can be seen in **Figure 6**, where the polymerized substrate shows significant cracks at three sides of the via, resulting in the via being not connected to the electrodes.

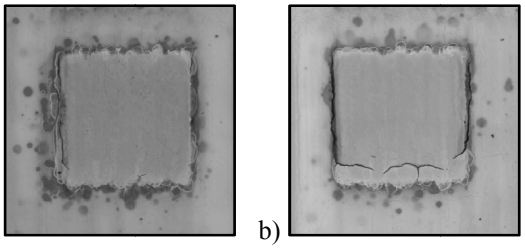

a) b)

Figure 6: *Vias and their cracking behaviour for (a) untreated and (b) polymerized substrates.*

The removed film is compensated by printing the lowest functional layer not in parallel but consecutive. Therefore firstly the $BaTiO_3$ is printed, forming a frame. This frame is then filled by printing the silver. All other functional layers are printed by applying both materials in parallel.

The functional improvement can be seen in **Figure 7**. Substrates were prefired at 300 °C, measured, and then fully fired at 850 °C and measured again. The untreated substrates show a largely decreased failure rate for their capacitors. It can further be seen, that the function is significantly determined in the firing at 300 °C which is done to burn out the organic additives. Here the silver shows already a large decrease in volume before the surface polymer is fully removed.

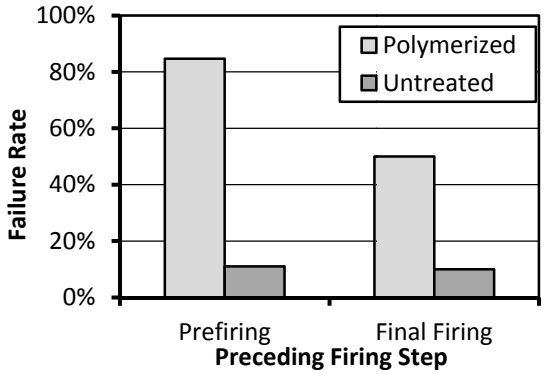

Figure 7: *Failure rates for capacitors.*

Pyrolysis

The priorfiring at 300 °C is necessary to remove the organic additives from the structure, that were added to the paste and the ink to create the rheologic properties needed for the printing process. It is important to burn out the organic additives before the silver sinters completely forming impenetrable layers.

Without priorprefiring, the volatile pyrolysis product will force their way through the sintered silver creating a dense pattern of cracks (**Figure 8**).

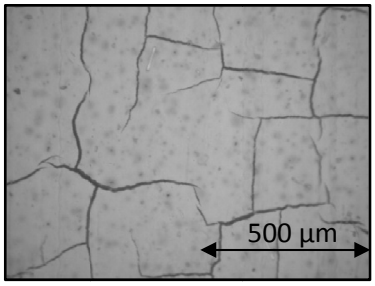

Figure 8: *Cracks caused by volatile pyrolysis products.*

To prevent these cracks, the organic additives have to be removed before the silver sinters completely. The used additive ethyl cellulose decays at normal atmosphere at temperatures of around 300 °C [11, 12].

Although the silver does reduce its volume in the priorfiring at 300 °C, as can be seen in the resulting cracks in Figure 6 b, it does not fully sinter (**Figure 9**). Although the sintering step at 300 °C greatly improves failure rates, due to the started sintering of silver the volatile pyrolysis products still causes some cracks.

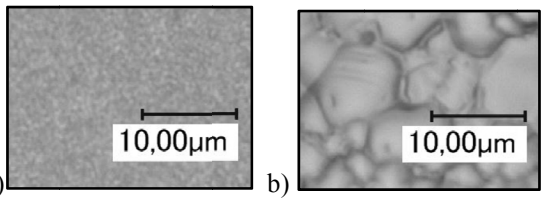

a) b)

Figure 9: *Microstructure of silver after (a) prefiring at 300 °C and (b) after sintering at 850 °C*

To solve the contradiction of the sintering temperature of 50 nm silver and the pyrolysis temperature of ethyl cellulosis it is tried to remove the ethyl cellulose by liquefying it. The used ethyl cellulose softens at 140 °C and melts at 170 °C [13].

Therefore an additional firing step is introduced, keeping the printed structure for 48 hours at 200 °C. In this process step, the printed particles may sediment in the liquefied ethyl cellulose resulting in much of the polymer accruing on top of the structure. Thus, firing later at 300 °C, the volatile pyrolysis products do not have to pass the silver layers reducing cracks and therefore the failure rate.

As can be seen in **Figure 10** the ethyl cellulose accrued on top of the printed structure, resulting in a paler appearance.

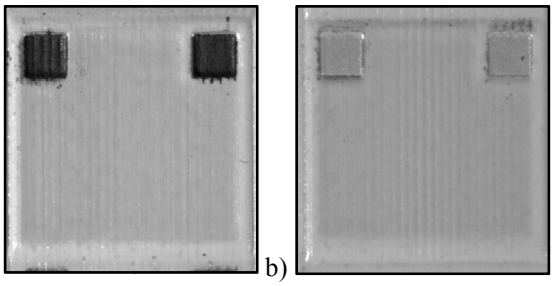

Figure 10: *Appearance of capacitor (a) after printing and (b) after prefiring at 200 °C*

However, this additional process step did not result in a decrease of failure rates but increased them further as can be seen in **Figure 11**.

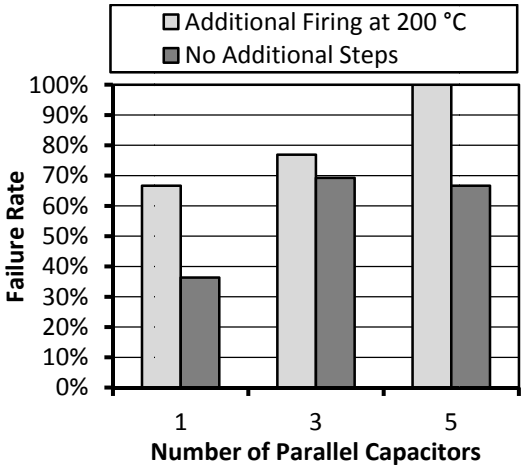

Figure 11: *Failure rates of capacitors applied to excessive pre-firing at 200 °C.*

This can be explained by particle movement. The reason why quick drying is advisable is that every liquid phase causes uncontrolled particle movement that can influence the geometric properties of the printed structure. Melting the organic additive for a prolonged period without burning it enables the printed particles to move uncontrolled. This effect offsets the possible gains of less volatile pyrolysis products inside the printed structure.

Capacitors

The RC-circuits capacitors are expected to follow the model derived in previous research [6]. This model contains a capacity and conductance for leak currents in a parallel circuit. It is expected for both the capacity of the capacitor

$$C_{\mathrm{tot}} = n_{\mathrm{c}} \cdot C_{\mathrm{cap}} \qquad (4)$$

and its conductance

$$G_{\mathrm{tot}} = n_{\mathrm{c}} \cdot G_{\mathrm{cap}} \qquad (5)$$

to increase linear with the number n_c of parallel capacitors [6].

This is, as can be seen in **Figure 12**, not the case. Both, average capacity and conductance behave rather randomly to the number of parallel capacitors but show a correlation towards each other.

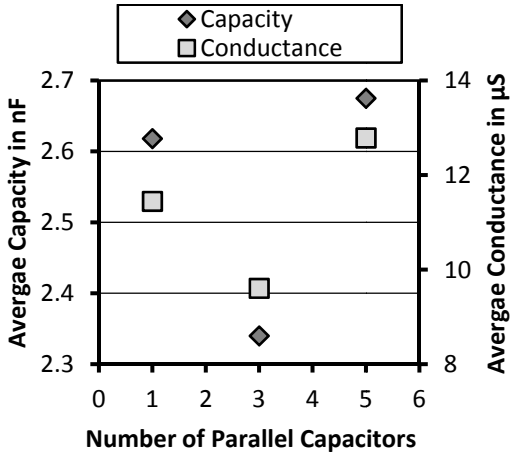

Figure 12: *Average capacity and conductance of 1-, 3- and 5-fold capacitors*

This correlation can clearly be shown by plotting conductance vs. capacity for individual capacitors (**Figure 13**) and is expected from (4) and (5) resulting in

$$G_{\mathrm{tot}} = \frac{G_{\mathrm{cap}}}{C_{\mathrm{cap}}} \cdot C_{\mathrm{tot}}. \qquad (6)$$

So although the actual conductance behaves randomly, it strongly correlates to the capacity. Additionally the capacity values are lower than expected from previous research.

The explanation lies in the drying induced vertical cracks. They curb the active area of the electrodes randomly thus creating smaller values. Due to the verticality of the cracks the height of the dielectric is not influenced. Thus the correlation of capacity and leak conductance remains.

This correlation shows that beyond the problem of drying induced cracks the printing of capacitors produces very consistent dielectric layers with very homogenous electrical behavior concerning both the capacity and the leak conductance.

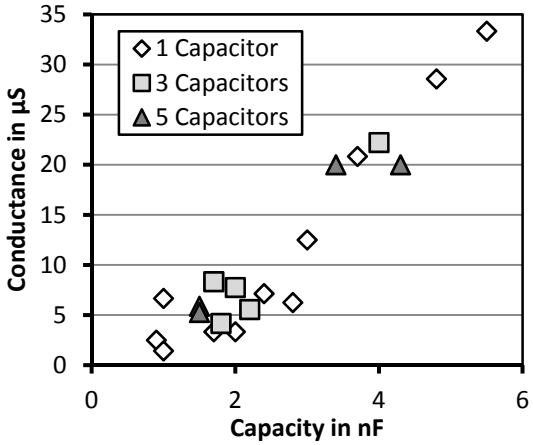

Figure 13: *Conductance and capacity for all sizes of capacitors.*

Resistors

The conductance of the resistors is expected to increase linearly with the number of printed layers and therefore the height and amount of applied ink. This is the mathematically most convenient way to model resistor behavior

$$G_{\mathrm{sq}} = n_{\mathrm{G}} \cdot \Delta h \cdot \sigma_{\mathrm{G}} \qquad (7)$$

with G_{sq} being the square conductance, n_{G} the number of printed layers, Δh the height of one layer and σ_{G} the conductivity of the printed material.

As can be seen in **Figure 14** the regression fits the measured values as expected.

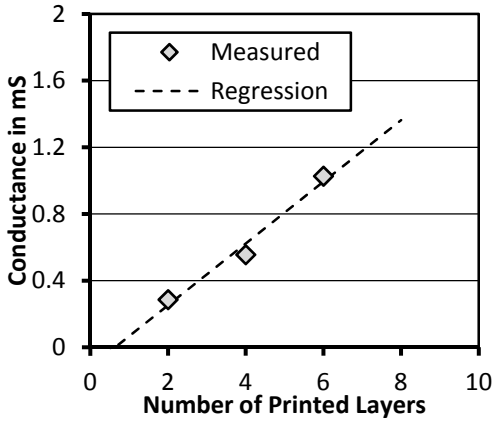

Figure 14: *Observed resistivity and regression model.*

Frequency Response

To evaluate the frequency behavior of the RC-circuits, the frequency response is measured. For a range from 1 kHz to 1 MHz the serial impedance of the RC-circuit is measured. The results can be seen in Figure 15, which shows the frequency Response for two RC-circuits with a similar capacity but different resistances. As expected, for lower frequencies behavior is determined by the capacity and for higher frequencies by resistance value.

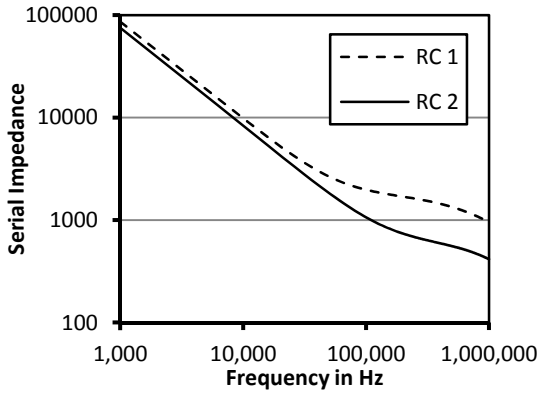

Figure 15: *Serial Impedance of different RC-Circuits.*

Summary and Outlook

To print RC-circuits the printing process was improved by closed-loop control of the most important process parameters. Furthermore a new silver ink was used to increase process stability. Thus a very stable process was achieved.

It could be shown that it is possible to manufacture RC-circuits using the inkjet process and that no firing between the different steps of printing is necessary.

Both capacitors and resistors behave as expected and in principle fit the models derived before.

The failure rate of the RC-circuits is still too high, with the drying process and the temperature incompatibility of the silver and the organic additives identified as causes for crack formation.

References

[1] D. Cibis, „Inkjet-Druckprozess zur Verarbeitung elektrisch funktioneller Tinten“, Dissertation Helmut-Schmidt-Universität, Hamburg 2009

[2] M. Waßmer, W. Diel, K. Krüger, „Inkjet printing of post-fired thick-film capacitors”, Proceedings of the 2009 Ceramic Interconnect and Ceramic Microsystems Technology (CICMT), pp. 33-38, Denver 2009

[3] M. Waßmer, W. Diel, K. Krüger, „Inkjet Printing of Thick-Film Resistors”, Proceedings of the 43rd International Symposium on Microelectronics (IMAPS), pp. 771-778, 2010

[4] D. Jeschke, K. Krüger, „In-Situ Blending of Inkjet-Printed Thick-Film Resistors“, Proceedings of the Ceramic Interconnect and Ceramic Microsystems Technology (CICMT), 2013

[5] M. Waßmer, „Inkjet-Druck passiver elektronischer Bauelemente“, Dissertation Helmut-Schmidt-Universität, Hamburg 2011

[6] D. Jeschke, E. Ahlfs, K. Krüger, „Inkjetprinting of Multilayer Capacitors“, Proceedings of the Ceramic Interconnect and Ceramic Microsystems Technology (CICMT), 2012

[7] M. Tseng, J. Jiao, „Design for Mass Customization by Developing Product Family Architecture”, Proceedings of DETC’98 ASME Design Engineering Technical Conferences, Atlanta, Georgia, 1998

[8] D. Cibis, K. Krüger, „System Analysis of a DoD Print Head for Direct Writing of Conductive Circuits”, International Journal of Applied Ceramic Technology , Volume 4, Issue 5, pp. 428-435, 2007

[9] Xaar, „Xaar 1001 Printhead User Manual”, Xaar Document No: D060208301 Version C

[10] U. Currle, „Funktionelle Partikeltinten für den Inkjet-Druck von mikroelektronischen Strukturen", Dissertation Helmut-Schmidt-Universität, Hamburg 2009
[11] F. Shafizadeh, „Industrial Pyrolysis of Cellulosic Materials", Proceedings of the Eighth Cellulose Conference, pp. 153-174, Syracuse, New York, Mai 19-23,1975
[12] R. Krausse, G. Behr, D. Schläfer, G. Krabbes, „Interactions between Ethylcellulose and thick-film resistors containing Ruthenium", Journal of Materials Science Letters 10, pp. 1392-1393, 1991
[13] Dow Chemical Company, „Ethocel – Ethylcellulose Polymers Technical Handbook", Dow Chemical Company, 2005